

# Purification, characterization, and spectral analyses of histidine-tagged vacuolar H<sup>+</sup>-pyrophosphatase expressed in yeast

Shen-Hsing HSU<sup>1</sup>, Yi-Yuong HSIAO<sup>2,3</sup>, Pei-Feng LIU<sup>1</sup>, Shih-Ming LIN<sup>1</sup>, Yue-Yu LUO<sup>1</sup>, and Rong-Long PAN<sup>1,\*</sup>

<sup>1</sup>*Department of Life Sciences and Institute of Bioinformatics and Structural Biology, College of Life Sciences, National Tsing Hua University, Hsin Chu 30043, Taiwan, Republic of China*

<sup>2</sup>*Department of Planning and Research, National Museum of Marine Biology and Aquarium, Pingtung 94450, Taiwan, Republic of China*

<sup>3</sup>*Institute of Marine Biotechnology, National Dong-Hwa University, Hualien 97401, Taiwan, Republic of China*

(Received September 1, 2008; Accepted March 27, 2009)

**ABSTRACT.** Vacuolar proton-translocating pyrophosphatase (V-PPase) generates a proton electrochemical gradient across the membrane by hydrolyzing pyrophosphate for maintenance of acidic condition of vacuoles and translocation of secondary metabolites, ions, and even toxics. The enzymatic activity of V-PPase could be stimulated by relatively high concentration of K<sup>+</sup>, but inhibited by F<sup>-</sup>, Na<sup>+</sup>, Ca<sup>2+</sup> and excess PP<sub>i</sub>. In this study, we used the yeast expression system to express hexa-histidine tagged mung bean V-PPase and employed detergent n-dodecyl β-D-maltoside (DDM) to solubilize the protein from microsomal membrane, followed by a Ni<sup>2+</sup>-nitrilotriacetate (Ni<sup>2+</sup>-NTA) affinity column to yield a highly purified enzyme. The specific activity of purified His-tagged V-PPase was approximately 86.4 ± 7.4 μmol PP<sub>i</sub> /mg.h, at least 6.5 fold purification compared to that on the vesicle membrane. The specific activity of His-tagged purified V-PPase were approximately 59% compare to the mung bean innate one. Further characterization indicates that the His-tagged V-PPase thus obtained resembles primarily those on membrane in most enzymatic features. The spectroscopic analyses including circular dichroism spectroscopy on His-tagged V-PPase revealed variations in conformational change induced by ions, as those inhibitors Na<sup>+</sup>, Ca<sup>2+</sup>, and F<sup>-</sup>, of this proton translocase. These results confirm the effect of ions are exerted concomitantly with the conformational (secondary structural) changes.

**Keywords:** Circular dichroism spectroscopy; Metal affinity chromatography; Vacuolar H<sup>+</sup>-pyrophosphatase; tonoplast.

**Abbreviations:** CD, circular dichroism; DDM, n-dodecyl β-D-maltoside; DTT, dithiothreitol; EDTA, N,N,N',N'-ethylene-diamine tetraacetic acid; EGTA, ethyleneglycol-bis (β-aminoethylether) N,N,N',N'-tetraacetic acid; Lyso-PC, L-α-lysophosphatidylcholine; PMSF, phenylmethylsulfonyl fluoride; PVDF, polyvinylidene difluoride; V-PPase, vacuolar H<sup>+</sup>-pyrophosphatase.

## INTRODUCTION

Vacuolar proton-translocating inorganic pyrophosphatase (V-PPase, EC 3.6.1.1)<sup>1</sup>, mainly found in higher plants, bacteria, archaea, and several protists, is an integral membrane protein that generates a proton electrochemical gradient across the membrane for secondary transport of solutes at expense of hydrolyzing pyrophosphate (Rea et al., 1992; Tzeng et al., 1996; Maeshima, 2000; Drozdowicz and Rea, 2001). V-PPase has been successfully purified from various sources and

was identified as a homodimer consisting of a single kind of polypeptide with a molecular mass of about 75-81 kDa (Wu et al., 1991; Maeshima, 2000; Yang et al., 2000). The cDNAs of V-PPase have been also cloned from several higher plants, protists, and prokaryotes (Rea et al., 1992; Hung et al., 1995; Maeshima, 2000; Drozdowicz and Rea, 2001) and analysis on deduced amino acid sequences showed 86 to 91% identity among higher plants and 36 to 39% between higher plants and *Rhodospirillum rubrum*, respectively (Rea et al., 1992; Maeshima, 2000; Drozdowicz and Rea, 2001). Furthermore, hydrophatic analysis predicts that V-PPase contains 14-16 transmembrane domains (Nakanishi et al., 2001; McIntosh and Vaidya, 2002; Mimura et al., 2004).

\*Corresponding author: E-mail: rlpan@life.nthu.edu.tw; Tel/ Fax: 886-3-5742688.

It was demonstrated that V-PPase requires  $Mg^{2+}$  as cofactor for enzymatic and proton translocation reactions (Gordon-Weeks et al., 1996; Maeshima, 2000). A line of evidence showed that the  $Mg^{2+}PP_i$  complex could protect the V-PPase from protease digestion (Nakanishi et al., 2001; Hsiao et al., 2004). Furthermore, the enzymatic activity of V-PPase could be stimulated by relatively high concentration of  $K^+$ , but substantially inhibited by  $F^-$ ,  $Na^+$ ,  $Ca^{2+}$  and excess  $PP_i$  (Walker and Leigh, 1981; Baltscheffsky and Baltscheffsky, 1993; Rea and Poole, 1993). As regards to  $K^+$  requirement, V-PPase was categorized into two subtypes, the  $K^+$ -dependent and  $K^+$ -independent V-PPases, respectively (Walker and Leigh, 1981; Baltscheffsky and Baltscheffsky, 1993; Drozdowicz and Rea, 2001). Recent study revealed that the V-PPase contained a  $K^+$  binding site at Ala-460 of V-PPase from *Carboxydotherrmus hydrogenoformans* and the replacement of this residue by Lys changed the phenotype of V-PPase from  $K^+$ -dependent to  $K^+$ -independent forms (Rea and Poole, 1993; Belogurov and Lahti, 2002). However, the domains accommodating other ions as well as its physiological regulators have not yet been determined.

From the amino acid alignment and site-directed mutagenesis studies, a highly conserved motif DX<sub>7</sub>KXE was suggested to be a putative substrate-binding site in the cytosolic loop between transmembrane domains 5 and 6 (Cooperman et al., 1992; Rea and Poole, 1993). It was further demonstrated that the two conserved acidic motifs (DX<sub>3</sub>DX<sub>3</sub>D) were involved in  $PP_i$  hydrolysis reaction (Maeshima, 1991; Rea et al., 1992; Hung et al., 1995; Baltscheffsky et al., 1999; Nakanishi et al., 2001). From chemical modification and site-directed mutagenesis studies, it was also shown that V-PPase possesses essential  $N,N'$ -dicyclohexylcarbodiimide (DCCD) binding acidic residues, presumably at Glu-305 and Asp-283 on cytosolic loop 3 and Asp-504 on cytosolic loop 5 (Yang et al., 1996; 1999; Zhen et al., 1997). A substrate protectable *N*-ethylmaleimid (NEM) modifiable Cysteine residue was identified at Cys-634 of V-PPase from *Arabidopsis thaliana* (Zhen et al., 1994; Kim et al., 1995). An essential histidine residue (His-716), presumably in the vicinity of active domain, was determined, for the inhibition of V-PPase by diethylpyrocarbonate (DEPC), a histidine specific modifier, would be removed by mutation at this histidine residue (Hsiao et al., 2004). Other essential amino acids and domains involved in enzymatic and proton translocation reactions are subjected to current investigations.

For further studies on the structure- function relationship of this proton translocating enzyme, a protocol for purification of heterologously expressed V-PPase is highly expected (Belogurov and Lahti, 2002; López-Marqués et al., 2005). In this communication, we report a successful method for solubilization and purification of a His-tagged mung bean V-PPase from the microsomal membrane of yeast. Several characteristics of purified

His-tagged V-PPase was investigated and compared to that on microsomal membrane. Furthermore, our results indicate that various ion effects on V-PPase are provoked via conformational changes as revealed by alterations in intrinsic fluorescence and circular dichroism (CD) spectra.

## MATERIALS AND METHODS

### Chemicals

Restriction endonucleases and T<sub>4</sub> DNA ligase were purchased from New England Biolabs (Beverly, MA, USA). Immunoblotting reagents were obtained from Bio-Rad (Hercules, CA, USA) and  $PP_i$  from Merck (Damstadt, Germany). All other chemicals were of analytic grade and used without further purification.

### Construction of His-tagged plasmid

The mung bean (*Vigna radiata* L. TN5) V-PPase cDNA (VPP; accession number P21616) (Hung et al., 1995) was cloned into the yeast expression vector pYES2 (Invitrogen, Carlsbad, CA, USA), and the synthesized oligonucleotide P<sub>his</sub> (5'-CCTCGAGCCATCATCATCATCAT TAG GGCCGCATCATGTAATTAGTTATGT-3') and P<sub>MluI</sub> (5'-GTACACGCGTCTGATCAG-3') were inserted into the 3'-end of the pYES2-VPP plasmid to generate the V-PPase-(His)<sub>6</sub> tail (Figure 1). The DNA sequence was then confirmed by DNA sequencing.

### Heterologous expression of V-PPase in yeast

The pYES2-VPP-(His)<sub>6</sub> cDNA was transferred into the *Saccharomyces cerevisiae* strain BJ2168 (*MATa*, *pre-407*, *prb1-1122*, *pep4-3*, *leu2*, *trp1*, *ura3*, *GAL*) according to the method described previously (Hsiao et al., 2004). The His-tagged V-PPase enriched yeast microsomal membrane was prepared as described by Kim et al. (Kim et al., 1995) with minor modifications (Hsiao et al., 2004). Four hundred milliliters of yeast cell culture in CM medium containing 0.5% (w/v) ammonium sulfate, 2% (w/v) glucose, 0.2% (w/v) yeast nitrogen base without amino acid and ammonium sulfate, 60  $\mu$ g/mL leucine, and 40  $\mu$ g/mL tryptophan were incubated at 30°C for 2 days and the yeast cells were pelleted down by centrifugation at 4,000 g for 10 min. The pellet was resuspended with 1 L CM medium with 2% (w/v) galactose to replace glucose for the induction of the V-PPase expression at 30°C for 3 days. The cells were collected by centrifugation at 4,000 g for 10 min and washed by incubating in 100 mM Tris/HCl (pH 9.4) and 100 mM dithiothreitol (DTT) at 37°C for 20 min with shaking at 150 rpm to remove peripheral fraction of V-ATPase from yeast vesicle membrane (Kane et al., 1989). After centrifugation at 4,000 g for 10 min, the cells were treated with lyticase in the medium containing 100 mM Tris/Mes (pH 8.0), 1% (w/v) yeast extract, 2% (w/v) peptone, 1% (w/v) glucose, 0.7 M sorbitol, 5 mM DTT, and 0.15% (w/v) lyticase (Sigma, St. Louis, Mo, USA) at 30°C with gentle shaking at 110 rpm for 2 h. After centrifugation at 4,000 g for 10 min, the spheroplasts were

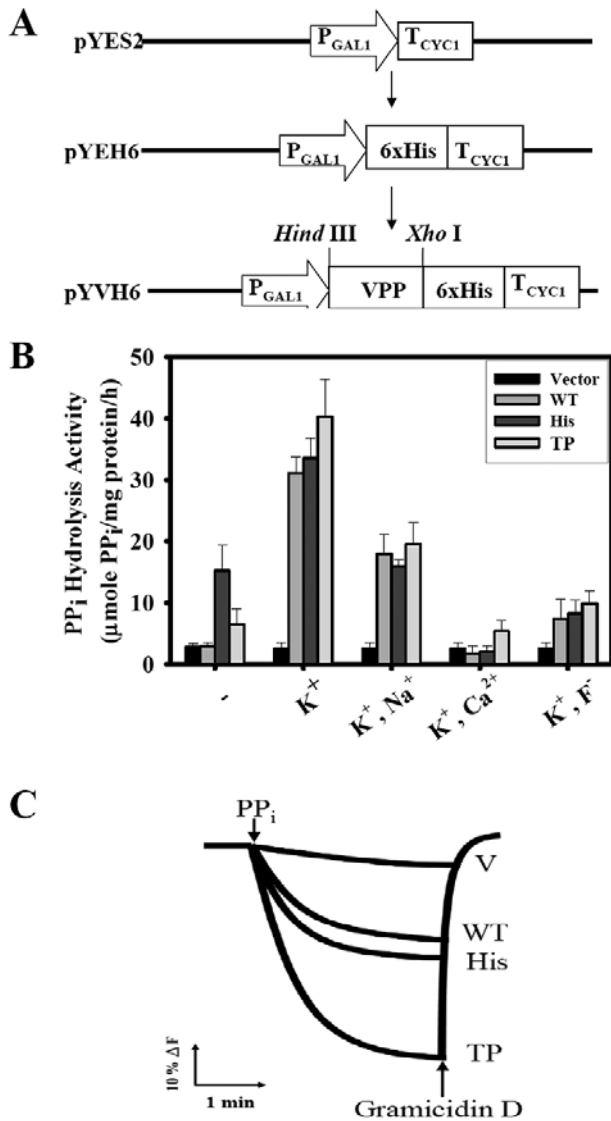


**Figure 1.** Heterologous expression of His-tagged mung bean V-PPase. (A) Construction of the vector containing His-tagged mung bean V-PPase. The yeast expression vector pYES2 was used as the PCR template. The 54-meric primer P<sub>His</sub> was designed to remove the *Xba*I restriction site and generate six histidine codons (CAT) followed by a new stop codon (TAG). The original *Xba*I-*Mlu*I fragment of the pYES2 vector was replaced by the *Xho*I-*Mlu*I fragment of the PCR product; (B) Enzymatic activities of innate and heterologously expressed His-tagged mung bean V-PPases. Microsomal vesicles containing WT and His-tagged V-PPase and V-PPase enriched tonoplast vesicles were isolated and enzymatic activities assayed according to the methods as described under "MATERIALS AND METHODS". The concentrations of ions, if present, were: 50 mM K<sup>+</sup>, 100 mM Na<sup>+</sup>, 0.1 mM Ca<sup>2+</sup>, and 20 mM F<sup>-</sup>, respectively; (C) Pyrophosphatase dependent H<sup>+</sup> translocation. PP<sub>i</sub> was added to initiate the proton translocation, and gramicidine D to stop the fluorescence quenching of acridine orange. V, WT, His, and TP represent microsomal vesicles from transformants with vector alone, wild type V-PPase, His-tagged V-PPase, and mung bean tonoplast, respectively.

resuspended in a medium containing 10% (w/v) glycerol, 5 mM Tris/Mes (pH 7.6), 50 mM Tris/ascorbate (pH 7.6), 2 mg/ml BSA, 1.5% (w/v) polyvinylpyrrolidone (M<sub>r</sub> 40,000), 1 mM PMSF, and 10 μg/ml pepstatin A. The spheroplasts were homogenized with a motor-driven Dounce homogenizer. After homogenization, the medium was pelleted down with 4,000 g for 10 min, and the precipitate was resuspended in the same medium, homogenized, and then centrifuged again. The supernatants were pooled together and centrifuged at 75,000 g for 1 h. The pellet was resuspended in suspension buffer containing 1.1 M glycerol, 1 mM Tris/EGTA, 5 mM Tris/Mes (pH 7.6), 2 mg/ml BSA, 2 mM DTT, 1 mM PMSF, and 10 μg/ml pepstatin A and then layered on to a discontinuous sucrose density gradient consisting of 10% (w/w) and 28% (w/w) sucrose in the suspension buffer. Following centrifugation at 75,000 g for 2 h, the V-PPase-enriched microsomes were withdrawn from the 10%/28% interface and diluted 10-fold by the storage buffer containing 5 mM Tris/Mes (pH 7.6) and 10% (w/v) glycerol. After centrifugation at 75,000 g for 55 min, the pelleted V-PPase-enriched membrane fractions were resuspended in the storage buffer and stored at -70°C for further use.

#### Purification of His-tagged V-PPase

The method for purifying His-tagged membrane protein was modified from procedure described by Lanfermeijer et al. (Lanfermeijer et al., 1998). The V-PPase (1 mg/mL) was solubilized in an extraction buffer containing 10 mM MOPS-KOH (pH 7.6), 400 mM KCl, 15% (w/v) glycerol, and 1 mM PMSF, and following by adding dropwise 10% (w/v) DDM to a final concentration of 0.5% and gently stirred for 30 min on ice. The solution was diluted with extraction buffer to 5 fold volume and unsolubilized materials were removed by centrifugation at 75,000 g at 4°C for 1 h. The supernatant was incubated with Ni<sup>2+</sup>-NTA (Ni<sup>2+</sup>-nitrilotriacetic acid) beads (Qiagen, Valencia, CA USA) pre-balanced with the extraction buffer containing 0.1% DDM. The Ni<sup>2+</sup>-NTA beads was injected into empty column and eluted at the flow rate of 0.5 mL/min with the elution medium containing 10 mM MOPS-KOH (pH 7.6), 15% (w/v) glycerol, 10 mM β-mercaptoethanol, 1 mM PMSF, and 0.1% DDM by step gradient of 20, 40, 60, and 250 mM imidazole, respectively. The fractions with highest PP<sub>i</sub> hydrolysis activity at 250 mM imidazole gradient were pooled and dialyzed against the medium containing MOPS-KOH (pH 7.6), 15% (w/v) glycerol, and 0.1% (w/v) DDM and then stored at -70°C for further studies.

#### Enzyme assay and protein determination

PPase activity was determined by measuring the release of P<sub>i</sub> from PP<sub>i</sub> as described previously (Hsiao et al., 2004). The reaction medium contained 30 mM Tris/Mes (pH 8.0), 1 mM MgSO<sub>4</sub>, 0.5 mM NaF, 50 mM KCl, 1 mM PP<sub>i</sub>, 1.5 μg/ml gramicidin D, and 20-30 μg/ml of microsome protein. For assaying purified His-tagged

protein, additional 0.1% (w/v) Triton X-100 and 80  $\mu\text{g}/\text{ml}$  phosphatidylcholine (soybean, type IV-S) were added in the reaction medium and 5  $\mu\text{g}$  purified protein included. The hydrolysis of pyrophosphate is linear with respect to concentration of V-PPase up to 300  $\mu\text{g}/\text{mL}$  and reaction time to 10-20 min under this condition at 37°C. After incubation the reaction was terminated by a stop solution containing 1.7% (w/v) ammonium molybdate, 2% (w/v) SDS, and 0.02% (w/v) 1-amino-2-naphthol-4-sulphonic acid. The released  $\text{P}_i$  was determined spectrophotometrically as described elsewhere (Fiske and Subbarow, 1925; Hsiao et al., 2004). For determination of optimal pH, different pH values of reaction media were maintained by adjusting pH value of Tris/Mes buffer. Lineweaver-Burk plots were obtained conventionally and values of  $K_M$  and  $V_{\text{max}}$  were thus determined using the SigmaPlot 5.0 software (SPSS, Chicago, IL, USA).

The concentration of the protein was measured by the dye-binding method of Bradford (Bradford, 1976) using BSA as standard or a modified Lowry method (Larson et al., 1986).

### Measurement of proton translocation

The fluorescence quenching of acridine orange (excitation wavelength 495 nm, emission wavelength 530 nm) was used to measure the proton translocation according to the method described previously (Hsiao et al., 2004). The reaction medium of proton translocation contained 5 mM Tris-HCl (pH 7.6), 1 mM EGTA/Tris, 400 mM glycerol, 100 mM KCl, 1.3 mM  $\text{MgSO}_4$ , 0.5 mM NaF, 5  $\mu\text{M}$  acridine orange, and 200  $\mu\text{g}/\text{mL}$  microsome protein. The proton translocation was initiated by adding 1 mM sodium pyrophosphate (pH 7.6) and terminated by the ionopore, gramicidin D (5  $\mu\text{g}/\text{mL}$ ). The initial fluorescence quenching of acridine orange was taken as the rate of proton translocation.

### SDS-PAGE and immunoblotting analysis

Polyacrylamide gel electrophoresis was performed according to Laemmli (Laemmli, 1970). The gels were stained with Silver Stain Kit (Bio-Rad) for visualization. For immunoblotting analysis, the gels were electrotransferred to polyvinylidene difluoride (PVDF) membrane using the Bandit™ Mini Tank Electroblot System with the transfer buffer containing 25 mM Tris (pH 8.5), 192 mM glycine, and 10% (v/v) methanol. The PVDF membrane was then blocked with 5% (w/v) skim milk in PBS-T buffer [10 mM  $\text{Na}_2\text{HPO}_4/\text{NaH}_2\text{PO}_4$  (pH 7.2), 150 mM NaCl, and 0.3% (w/v) Tween 20], with gently shaking at 4°C for 2 h. The PVDF membrane was incubated by gently shaking with the mouse polyclonal antibody raised against the KLH (Keyhole limpet hemocyanin) conjugated synthetic peptide of the sequence C<sup>715</sup>HKA AVIGDTIGDPLK<sup>730</sup> of the mung bean V-PPase as the primary antibody or anti-His-tagged antibody at 4°C for 2 h. After wash, the PVDF membrane was incubated with anti-mouse IgG-conjugated horseradish peroxidase in

PBS-T buffer containing 5% (w/v) skim milk at 4°C for 2 h. After washing with PBS-T buffer 4 times, the antibodies bound to antigen were detected with chemiluminescent reagents (Western blotting detection reagent, NEN™ Life Science Product).

### Spectral measurements

The intrinsic absorption spectra of the purified His-tagged V-PPase were determined with a Hitachi U2000 spectrophotometer (Hitachi, Ltd., Tokyo, Japan) in a medium containing 10 mM Tris-HCl (pH 8.0) and 15% (w/v) glycerol, and 10  $\mu\text{M}$  purified V-PPase. The intrinsic fluorescence spectra of purified V-PPase (10  $\mu\text{M}$ ) were determined in the same medium with a Hitachi F-4000 fluorophotometer using excitation wavelength of 273 nm. Secondary structure of purified V-PPase (7.5  $\mu\text{M}$ ) was determined at 25°C on a AVIV 202 spectropolarimeter (Aviv Associates, Lakewood, NJ) using quartz cells with 0.1 cm pathlength in a wavelength range between 200 and 260 nm (Yang et al., 2004). His-tagged V-PPase was dialyzed against 50 mM Tris-HCl (pH 7.2) and 1 mM DTT. The resultant spectra were corrected for the buffer signal. CD spectra shown were averages of at least three scans for each sample. The contents of secondary structure were calculated according to the method of Gans et al. (Gans et al., 1991).

### Ion contamination in reaction media

The background concentrations of  $\text{K}^+$ ,  $\text{Na}^+$ , and  $\text{Ca}^{2+}$  were determined by ICP-MS (Inductively coupled plasma-mass spectrometer) at NTHU Instrument Center, National Tsing Hua University, Hsin Chu, Taiwan, as 0.13, 0.6, and 0.98  $\mu\text{M}$ , respectively.

## RESULTS AND DISCUSSION

### Expression and purification of mung bean V-PPase in yeast

The cDNA encoding mung bean vacuolar  $\text{H}^+$ -PPase was constructed with His-tagged tail at C-terminus and incorporated into *E. coli/S. cerevisiae* expression shuttle vector pYES2 (Figure 1). The vacuolar protease-deficient yeast strain BJ2168 was used for heterologous expression of His-tagged mung bean V-PPase and the desired protein was then transcribed efficiently in yeast under the control of the promoter of *GALI* (Kim et al., 1995; Hsiao et al., 2004). His-tagged V-PPase-enriched membranes were successfully prepared by sucrose gradient centrifugation and then subjected to SDS-PAGE and immunoblotting with polyclonal antibodies specific to the deduced substrate-binding site of V-PPase (Figure 2A, lane 2) (Nakanishi et al., 2001). The results were further confirmed by anti-His-tagged antibody (data not shown). The His-tagged V-PPase enriched fraction produced primarily a band with molecular mass of 73-kDa that could be solely recognized by antibodies. The partially purified V-PPase enriched microsome and mung bean tonoplast

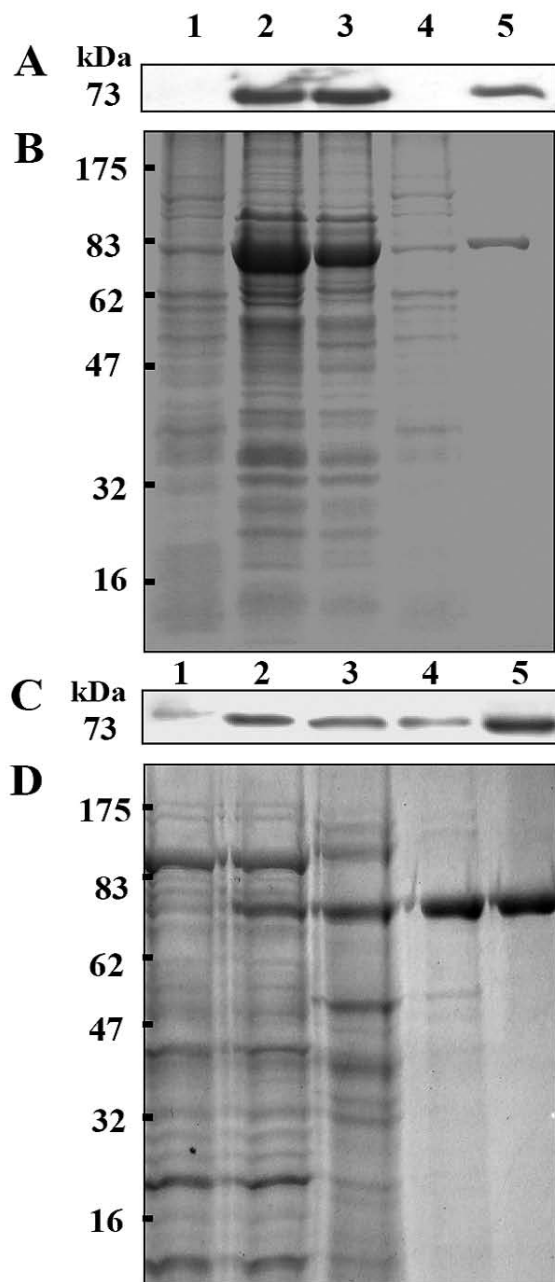


**Figure 2.** SDS-PAGE and immuno-blotting analysis of purified V-PPase. The different fractions from each step were isolated and subjected to SDS-polyacrylamide gel electrophoresis (B) and immunoblotting analysis (A). Lane 1, pYES2 vector as the negative control; lane 2, microsomal membrane enriched in heterologously expressed V-PPase; lane 3, the supernatant from DDM (0.5% (w/v)) extraction; lane 4 and 5, fractions eluted from Ni<sup>2+</sup>-NTA column by 20 and 250 mM imidazole, respectively. The molecular mass of His-tagged V-PPase is about 73 kDa. Standard molecular masses are shown on the left-hand side of the gels. The fractions from each purification step were eluted and subjected to SDS-polyacrylamide gel electrophoresis (D) and immunoblotting analysis (C). Lane 1, the tonoplast membrane from mung bean hypocotyl tissues; lane 2, the supernatant from DDM (0.5% (w/v)) extraction; lanes 3, 4, and 5, fractions eluted from DEAE, Sephacryl S-200, and Mono-Q chromatographies, respectively.

displayed PP<sub>i</sub> hydrolysis and PP<sub>i</sub>-associated proton translocation (Figure 1B, C), whereas that transformed by pYES2 alone showed only negligible PPase activities and proton translocation. The PP<sub>i</sub> hydrolysis reaction could be stimulated 7-10 fold by 50 mM KCl, but substantially inhibited by 20 mM NaF, 100 mM NaCl, and 0.1 mM CaCl<sub>2</sub> to appropriate extents, respectively (Figure 1B). Moreover, the PP<sub>i</sub>-dependent pH gradient could be collapsed by addition of ionophore, gramicidin D, indicating the integrity of microsomal membranes and the electrogenic H<sup>+</sup>-transport in vesicles (Figure 1C). These results demonstrated that the expressed protein is in a good agreement with mung bean V-PPase and expression system is feasible for following studies.

His-tagged V-PPase was solubilized from microsomal membrane preparation using different detergents. Firstly, the membrane fraction was subjected to Lyso-PC (L- $\alpha$ -lysophosphatidylcholine), a detergent conventionally used to solubilize the V-PPase from tonoplast (Maeshima and Yoshida, 1989), and then applied to a Ni<sup>2+</sup>-NTA column. However, the PP<sub>i</sub> activity was detected only at flow-through fraction (data not shown). The presence of Lyso-PC obviously disturbed the binding of His-tagged V-PPase to Ni<sup>2+</sup>-NTA column. Other detergents, such as Triton X-100, octylglucopyranoside, and Brij 35, were then tried in vain to appropriately solubilize V-PPase from microsomal membrane fraction (data not shown). Alternatively, we employed DDM (n-dodecyl  $\beta$ -D-maltoside) to solubilize His-tagged V-PPase from microsomal membrane and the supernatant could successfully bind to Ni<sup>2+</sup>-NTA column (Lanfermeijer et al., 1998). In a similar way, DDM was also used to solubilize innate mung bean V-PPase from tonoplast membrane without any significant effects on the enzymatic activity (Figure 1B). DDM was thus routinely utilized for the solubilization of V-PPases from microsomal membranes of expressing yeast as well as from those of mung bean tonoplast. The optimal condition for DDM to solubilize His-tagged V-PPase was at 0.5% (w/v) for 30 min incubation time. However, prolong incubation and higher concentration induced the demolishment of the enzymatic activity of His-tagged V-PPase (data not shown). Following appropriate incubation with DDM and binding of solubilized fraction to the Ni<sup>2+</sup>-NTA column, imidazole gradient was then used to elute the protein from the column. His-tagged V-PPase was primarily eluted from the column at the imidazole concentration of 250 mM. According to this purification procedure, a clear single band with a molecular mass of about 73 kDa was visualized on SDS-PAGE and recognized by anti-V-PPase (Figure 2A, lane 5) and anti-His-tagged (data not shown) antibodies. Therefore, 0.5% (w/v) DDM was routinely used for solubilization of His-tagged and innate mung bean V-PPases in following studies. Table 1 summarizes the results from each step of purification of His-tagged (Table 1A) and innate mung bean V-PPases (Table 1B). The specific activity of purified His-tagged V-PPase was approximately  $86.4 \pm 7.4$   $\mu\text{mol PP}_i/\text{mg.h}$ , at least 6.5 fold

purification as compared to  $13.3 \pm 4.5 \mu\text{mol PP}_i/\text{mg.h}$  of that on the vesicle membrane. The specific activity of purified His-tagged V-PPase was only about 59% of that directly purified from mung bean (i.e.,  $147.5 \pm 4.3 \mu\text{mol PP}_i/\text{mg.h}$ , Table 1B). The reason for lower specific activity of the purified His-tagged V-PPase than that of mung bean requires more elucidations. Nevertheless, our expression system and purification protocols suffice to provide a highly purified His-tagged V-PPase for further investigations.

### Kinetic parameters and optimal pH of purified His-tagged V-PPase

Table 2 summarized the kinetic parameters of various types V-PPase. Conventional Lineweaver-Burk analysis

gave apparent  $K_M$  and  $V_{max}$  values of  $71.9 \pm 2.8 \mu\text{M}$  and  $38.0 \pm 1.3 \mu\text{mol PP}_i/\text{mg.h}$  for wild type V-PPase on microsomal membrane, respectively. Furthermore, the  $K_M$  and  $V_{max}$  values of purified V-PPase from mung bean were  $297.6 \pm 13.4 \mu\text{M}$  and  $291.4 \pm 5.6 \mu\text{mol PP}_i/\text{mg.h}$  (Table 2, Yang et al., 1999). Similarly, apparent  $K_M$  values of  $242.3 \pm 5.7$  and  $115.0 \pm 3.0 \mu\text{M}$  and the apparent  $V_{max}$  values of  $302.5 \pm 11.3$  and  $72.5 \pm 3.4 \mu\text{mol PP}_i/\text{mg.h}$  were determined for solubilized and membrane bound His-tagged V-PPases, respectively (Table 2). The  $K_M$  values of His-tagged V-PPase, in either membrane-bound or solubilized states, are larger than that of the wild type V-PPase on microsomal membrane, indicating that the affinity of their substrates is decreased upon the attachment of His-tagged tail to the C-terminus of the enzyme.

**Table 1.** Summary of purification of heterologously expressed His-tagged V-PPase from yeast microsomal membrane and innate mung bean V-PPase from tonoplast membrane. Yeast microsomal membranes and mung bean tonoplast membranes were prepared and  $\text{PP}_i$  hydrolysis determined according to the methods as described under "MATERIALS AND METHODS". The V-PPase enriched membranes were solubilized by 0.5% DDM for 30 min on ice. The solubilized fractions containing His-tagged V-PPase were then subjected to  $\text{Ni}^{2+}$ -NTA column and the purified V-PPase was finally eluted by 250 mM imidazole. The solubilized fractions containing mung bean innate V-PPase were then subjected to DEAE-column, followed by Sephacryl S200 as the second, and Mono-Q, the third columns, to yield the purified innate mung bean V-PPase. Values were means  $\pm$  S.D. from at least 3 independent experiments.

Purification steps	Total protein (mg)	V-PPase activity			Purification (Fold)
		Specificity activity ( $\mu\text{mol PP}_i/\text{mg.h}$ )	Total activity ( $\mu\text{mol PP}_i/\text{mg.h}$ )	Recovery (%)	
(A) Heterologously expressed His-tagged V-PPase from yeast microsomal membrane					
Membrane fraction	$30.5 \pm 4.4$	$13.3 \pm 4.5$	$405.7 \pm 149.2$	100.0	1.0
DDM extraction	$23.4 \pm 3.2$	$15.1 \pm 3.3$	$353.3 \pm 91.1$	87.1	1.1
$\text{Ni}^{2+}$ -NTA elution	$1.2 \pm 0.1$	$86.4 \pm 7.4$	$103.7 \pm 12.4$	25.6	6.5
(B) Innate mung bean V-PPase from tonoplast membrane					
Membrane fraction	$100.5 \pm 6.2$	$24.4 \pm 2.5$	$2452.2 \pm 293.3$	100.0	1.0
DDM extraction	$72.3 \pm 5.4$	$31.3 \pm 5.5$	$2263.0 \pm 432.1$	92.3	1.3
DEAE column	$41.4 \pm 4.3$	$48.7 \pm 3.7$	$2016.2 \pm 259.5$	82.2	2.0
S-200 column	$8.3 \pm 2.5$	$82.4 \pm 5.4$	$683.9 \pm 210.8$	27.9	3.4
Mono-Q column	$1.7 \pm 0.4$	$147.5 \pm 4.3$	$250.6 \pm 59.5$	10.2	6.0

**Table 2.** Kinetic parameters of various types of V-PPases. V-PPases of each type were isolated and their enzymatic activities determined as described under "MATERIALS AND METHODS". For determination of optimal pH, different pH values of reaction media were maintained by adjusting pH value of Tris-Mes buffer. Lineweaver-Burk plots were obtained conventionally and values of  $K_M$  and  $V_{max}$  were thus calculated using the SigmaPlot 5.0 software (SPSS, Chicago, IL, USA). The concentrations of ions, if present, were: 50 mM  $\text{K}^+$ , 100 mM  $\text{Na}^+$ , 0.1 mM  $\text{Ca}^{2+}$ , and 20 mM  $\text{F}^-$ , respectively. Values were means  $\pm$  S.D. from at least 3 independent experiments.

V-PPase	$K_M$ ( $\mu\text{M}$ )	$V_{max}$ ( $\mu\text{mol PP}_i/\text{mg.h}$ )	Optimum pH	Ion stimulation (Fold)		Ion inhibition (%)		
				$\text{K}^+$		$\text{Na}^+$	$\text{Ca}^{2+}$	$\text{F}^-$
WT/Membrane-bound	$71.9 \pm 2.8$	$38.0 \pm 1.3$	8.2	10.7		58.1	5.8	24.8
His-tagged/Membrane-bound	$115.0 \pm 3.0$	$72.5 \pm 3.4$	8.2	2.2		47.7	6.0	24.7
His-tagged/Purified	$242.3 \pm 5.7$	$302.5 \pm 11.3$	8.3	2.4		47.1	6.7	24.7
Innate/Purified	$297.6 \pm 13.4$	$291.4 \pm 5.6$	8.2	8.4		61.3	5.9	24.5

However, the  $V_{\max}$  of His-tagged V-PPase on membrane vesicle is approximately two fold of wild type. The presence of extra 6 histidine residues at the C-terminus of V-PPase presumably stimulates the reactivity of the enzyme in spite the fact that the accessibility of substrate is decreased. Evidence showed that C-terminus of V-PPase might locate in the vicinity of its active site and is crucial to the structure and consequently to both enzymatic and proton-translocating reactions of the enzyme (Takasu et al., 1997). The extension of C-terminus by His-tagged tail might bring about the conformational variations, resulting in the changes in the accessibility of the substrate to active domain and reactivity of V-PPase. The role of C-terminus and exact effect of His-tagged tail on V-PPase deserve our further investigations.

Furthermore, pH profiles of PP<sub>i</sub> hydrolysis activities were scrutinized for various types of V-PPases, including wild type and His-tagged V-PPases on microsomal membranes, and purified His-tagged and purified mung bean V-PPases. All of these three types of V-PPase showed similar optimal pH values at 8.2-8.3, respectively (Table 2). Obviously, the presence of His-tagged tail in the C-terminus of V-PPase did not provoke any significant difference in their optimal pH values, even that His-tagged tail might induce modification of  $K_M$  and  $V_{\max}$  values as shown above.

### Ion effects on His-tagged V-PPase

Mg<sup>2+</sup> is absolutely required for enzymatic activity of V-PPase by forming a complex with its physiological substrate as Mg<sup>2+</sup>PP<sub>i</sub>. In the presence of 1 mM PP<sub>i</sub>, the maximal activity of V-PPase was obtained at concentration of 1 mM Mg<sup>2+</sup>, above which the enzymatic activity was gradually decreased (data not shown). The Mg<sup>2+</sup>PP<sub>i</sub> complex protected V-PPase from protease degradation (Maeshima, 1991; Rea and Poole, 1993; Gordon-Weeks et al., 1996). Nevertheless, it has been suggested that the V-PPase contain two Mg<sup>2+</sup> binding site in distinct regions, with one of them for low affinity and the other for high affinity (Baykov et al., 1993; Zhen et al., 1997; Maeshima, 2000). Furthermore, K<sup>+</sup> is also an essential cofactor of V-PPase and could stimulate its enzymatic and proton translocating reactions (Obermeyer et al., 1996; Zhen et al., 1997). The activities of wild type V-PPase on microsomal membrane and purified innate one reached maximal at concentration of K<sup>+</sup> above 50 mM, yielding an approximately 8-10 fold increase in enzymatic reaction (Table 2). However, upon the attachment of His-tagged tail at C-terminus of V-PPase, the extent of stimulation was decreased to 2-3 fold. Moreover, after purification of His-tagged V-PPase from microsomal membrane, the degree of K<sup>+</sup>-stimulation still remained on 2-3 fold. It is conceivable that wild type and His-tagged enzyme display similar activities in the presence of 50 mM K<sup>+</sup> but the His-tagged tail renders V-PPase significantly active in the absence of K<sup>+</sup>. In contrast, activity of the wild type preparation is indistinguishable from that of control preparation without

V-PPase in the absence of K<sup>+</sup> (Figure 1B). Moreover, our recent truncation analysis revealed that the deletion of 10 amino acids in C-terminal region lead to similar decrease in the K<sup>+</sup> stimulation of V-PPase activity (Lin et al., 2005). It is possible that the C-terminal domain is directly or indirectly involved in the K<sup>+</sup> regulation of V-PPase. On the other hand, it has been successfully demonstrated that Lys-460 of V-PPase from *C. hydrogeniformans* might be the site for K<sup>+</sup> binding (Belogurov and Lahti, 2002). We thus speculate that this binding site of K<sup>+</sup> at V-PPase may locate in the vicinity of C-terminal region; consequently its modification by His-tagged tail provokes the decrease in the K<sup>+</sup>-stimulation of the enzyme. Alternatively, the K<sup>+</sup> binding site might not be near the V-PPase C-terminus and we cannot exclude the possibility that the His-tag of C-terminus induces conformational change to increase the K<sup>+</sup> stimulation.

In contrast, enzymatic activity of V-PPase could be abolished in the presence of Na<sup>+</sup>, Ca<sup>2+</sup>, and F<sup>-</sup>, respectively (Maeshima, 2000; Rea et al., 1992). In general, the V-PPase on the vesicle membrane could be inhibited by Ca<sup>2+</sup> with half-maximal inhibition values ( $I_{50}$ ) at 37.2 μM. At the concentration of Ca<sup>2+</sup> higher than 300 μM, the enzymatic activity of V-PPase was brought to 5.8% of the control (Table 2). Moreover, enzymatic activities of the His-tagged V-PPases were decreased to similar extents by Ca<sup>2+</sup>, regardless in purified form or on microsomal membrane. Obviously, the presence of His-tagged tail did not result in any difference in the sensitivity of V-PPase to Ca<sup>2+</sup>. Furthermore, Na<sup>+</sup> could inhibit wild type V-PPase on vesicle membrane to 58.1% at concentration of 100 mM. Similar effects were observed for the His-tagged V-PPases either in membrane-bound or purified states. In addition, F<sup>-</sup> could inhibit wild type V-PPase activity to 24.8% at concentration of 20 mM. Likewise, the relative activities of His-tagged V-PPases were reduced to approximately 24.7% of those in the absence of F<sup>-</sup>. In short, the extents of ion inhibition on enzymatic activities of various types of V-PPase are similar, despite that the stimulation of enzyme by K<sup>+</sup> is partially removed upon His-tagging at its C-terminal domain.

### Spectroscopic properties of purified His-tagged V-PPase

The spectral properties of purified His-tagged V-PPase and purified innate mung bean in the presence of different ions were observed. The intrinsic absorption did not show any significant change in the presence of different concentrations of ions mentioned above, respectively (Figure 3A). However, the intrinsic fluorescence of V-PPase was progressively increased with the increase in Ca<sup>2+</sup> concentration and reached to 2.1 fold at 5 mM of Ca<sup>2+</sup> (Figure 3B, —•—). Figure 3B displays the variation in intensities of intrinsic fluorescence of purified V-PPase upon the presence of various ions. In general, the fluorescence intensities of purified V-PPase were increased by each ion scrutinized with more obvious changes by Ca<sup>2+</sup>

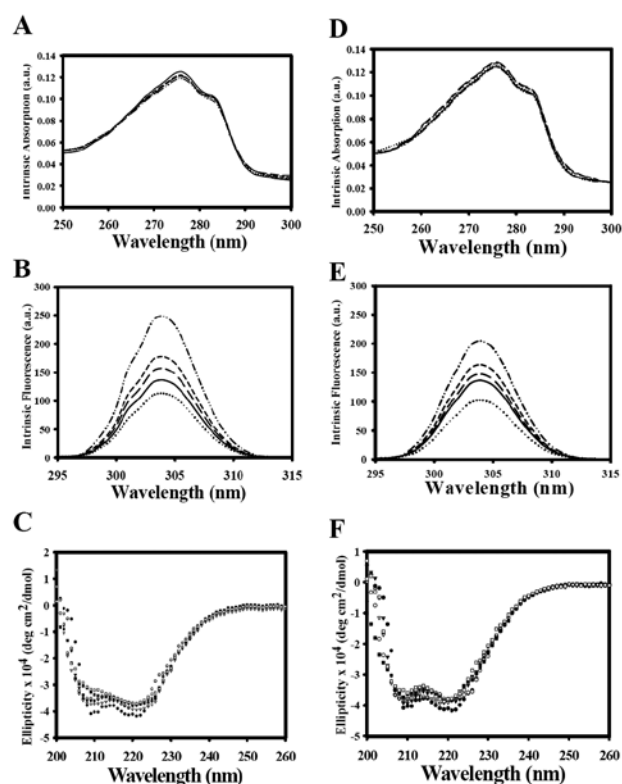


**Figure 3.** The spectra of purified His-tagged and innate mung bean V-PPases. (A, D) Intrinsic absorption. The medium contained 10  $\mu$ M purified His-tagged and innate mung bean V-PPases, 10 mM Tris/HCl (pH 8.0), 15% (w/v) glycerol, and various ions. The concentrations of ions, if present, were: 50 mM  $K^+$ , 100 mM  $Na^+$ , 0.1 mM  $Ca^{2+}$ , and 20 mM  $F^-$ , respectively. The scanning was carried out in the range from 250 to 300 nm at 25°C. (B, E) Intrinsic fluorescence. The excitation wavelength was 273 nm and emission wavelength was scanned from 295 to 315 nm, respectively. The medium and ions are the same as in intrinsic absorption measurements. (C, F) CD spectra. The medium contained 7.5  $\mu$ M purified His-tagged and innate mung bean V-PPases, 50 mM Tris/HCl (pH 7.2), 1 mM DTT, and the various ions as indicated above. The scanning was carried out in the range from 260 to 200 nm at 25°C. (—), control; (— —),  $K^+$ ; (—•—),  $Na^+$ ; (—••—),  $Ca^{2+}$ ; (•••),  $F^-$ .

and  $Mg^{2+}$  than  $K^+$ . The binding of these ions may induce conformational changes of V-PPase, consequently leaving the intrinsic fluorophores in a more favorable environment for fluorescence.

The CD spectra were then used to analyze the secondary structure of 6x His-tagged V-PPase (Figure 3C). The CD curve reveals that 6x his V-PPase is a typical protein with 44.5%  $\alpha$ -helix, 33.5% random coil, and 19.0%  $\beta$ -sheet, respectively (Table 3). The  $\alpha$ -helix content of His-tagged V-PPase is lower than that of purified mung bean V-PPase (Yang et al., 2004), probably due to the His-tagged tail and different techniques employed. Moreover, we can not exclude the possibility that the difference in secondary structure of innate and heterologous expressed V-PPases might come from the distinct expression systems (Liu et al., 2005). Nevertheless, the CD spectra of V-PPase were modified in the presence of ions as indicated in the vicinity of both troughs around 210 and 220 nm, respectively (Figure 3C). Accordingly, the presence of  $K^+$  slightly increases the content of  $\alpha$ -helix but decreases that of  $\beta$ -sheet. In contrast, inhibitory ions (i.e.,  $Na^+$ ,  $Ca^{2+}$ , and  $F^-$ ) substantially decrease content of  $\alpha$ -helix and inversely, increase those of  $\beta$ -sheet. These results confirm the effect of ions is exerted concomitantly with the conformational (secondary structural) changes. The structure variation of V-PPase upon the binding of these ions deserves our further investigations.

## Conclusions and outlook

Vacuolar proton translocating inorganic pyrophosphatase plays a critical role in secondary transport of solutes in higher plants, bacteria, archaea, and many protists (Maeshima, 2000; Drozdowicz and Rea, 2001). Phylogenetic analysis reveals V-PPases from various sources may derive from common ancestors. The discovery of V-PPase in many parasitic protists but not their animal hosts renders this enzyme as a drug target by rational design for many specific diseases of public concerns. Thus a proper protocol to purify V-PPase with high homogeneity for direct observation of its structure

**Table 3.** Contents of secondary structure of V-PPase in the presence of various ions. CD spectra of purified V-PPase was determined in a medium containing 7.5  $\mu$ M purified His-tagged and innate mung bean V-PPase, 50 mM Tris/HCl (pH 7.2), 1 mM DTT, and the various ions as indicated at 25°C, respectively. The concentrations of ions, if present, were: 50 mM  $K^+$ , 100 mM  $Na^+$ , 0.1 mM  $Ca^{2+}$ , and 20 mM  $F^-$ , respectively. The contents of secondary structure were calculated according to the method of Gans et al. (Gans et al., 1991).

Additions	$\alpha$ -Helix (%)		$\beta$ -Sheet (%)		$\beta$ -Turn (%)		Random-coil (%)	
	His-tagged	Innate	His-tagged	Innate	His-tagged	Innate	His-tagged	Innate
Control	44.5	55.8	19.0	21.4	3.0	3.4	33.5	19.4
+ $K^+$	49.8	56.9	14.6	17.6	3.1	3.8	32.5	21.7
+ $Na^+$	33.2	51.4	26.6	25.4	4.6	3.5	35.7	19.7
+ $Ca^{2+}$	35.7	51.2	23.1	24.3	6.1	4.5	35.2	20.0
+ $F^-$	33.9	52.3	24.7	22.7	6.5	4.1	34.9	20.9

and function would be appreciated for workers on this enzyme. In this study, we used the yeast *S. cerevisia* expression system, originally developed by Kim et al. (Kim et al., 1995) to generate 6x His-tagged mung bean V-PPase and employed detergent DDM to solubilize the protein from microsomal membrane, followed by a Ni<sup>2+</sup>-NTA affinity column to obtain a highly purified enzyme. The His-tagged V-PPase thus obtained resembles primarily those on membrane in most enzymatic features, favoring its further structural studies. The spectroscopic analyses on His-tagged V-PPase provide a means to observe the variation in conformational changes induced by several ions long known as inhibitors of this novel proton translocase. Further studies on structure-function relationship of V-PPase obtained by this expression system and purification protocol to get high purity and large amount of protein for x-ray crystal structure analysis are currently undertaken in this laboratory.

**Acknowledgements.** This work was supported by the grant from National Science Council, Republic of China (NSC 97-2311-B-007-002 and 97-2627-M-007-003) to RLP.

## LITERATURE CITED

- Baltscheffsky, M. and H. Baltscheffsky. 1993. Inorganic pyrophosphate and inorganic pyrophosphatase. *In: Molecular mechanisms in bioenergetics*, Elsevier, Amsterdam, pp. 331-348.
- Baltscheffsky, M., A. Schultz, and H. Baltscheffsky. 1999. H<sup>+</sup>-PPases: a tightly membrane-bound family. *FEBS Lett.* **457**: 527-533.
- Baykov, A.A., E.B. Dubnova, N.P. Bakuleva, O.A. Evtushenko, R.G. Zhen, and P.A. Rea. 1993. Differential sensitivity of membrane-associated pyrophosphatases to inhibition by diphosphonates and fluoride delineates two classes of enzyme. *FEBS Lett.* **327**: 199-202.
- Belogurov, G.A. and R. Lahti. 2002. A lysine substitute for K<sup>+</sup>. A460K mutation eliminates K<sup>+</sup> dependence in H<sup>+</sup>-pyrophosphatase of *Carboxydotherrmus hydrogenoformans*. *J. Biol. Chem.* **277**: 49651-49654.
- Bradford, M.M. 1976. A rapid and sensitive method for the quantitation of microgram quantities of protein utilizing the principle of protein-dye binding. *Anal. Biochem.* **72**: 248-254.
- Cooperman, B.S., A.A. Baykov, and R. Lahti. 1992. Evolutionary conservation of the active site of soluble inorganic pyrophosphatase. *Trends Biochem. Sci.* **17**: 262-266.
- Drozdowicz, Y.M. and P.A. Rea. 2001. Vacuolar H<sup>+</sup>-pyrophosphatases: from the evolutionary backwaters into the mainstream. *Trends Plant Sci.* **6**: 206-211.
- Fiske, C.H. and Y. Subbarow. 1925. The colorimetric determination of phosphorous. *J. Biol. Chem.* **66**: 378-400.
- Gans, P.J., P.C. Lyu, M.C. Manning, R.W. Woody, and N.R. Kallenbach. 1991. The helix-coil transition in heterogeneous peptides with specific side-chain interactions: theory and comparison with CD spectral data. *Biopolymers* **31**: 1605-1614.
- Gordon-Weeks, R., S.H. Steele, and R.A. Leigh, 1996. The role of magnesium, pyrophosphate, and their complexes as substrates and activators of the vacuolar H<sup>+</sup>-pumping inorganic pyrophosphatase (Studies using ligand protection from covalent inhibitors). *Plant Physiol.* **111**: 195-202.
- Hsiao, Y.Y., R.C. Van, S.H. Hung, H.H. Lin, and R.L. Pan. 2004. Roles of histidine residues in plant vacuolar H<sup>+</sup>-pyrophosphatase. *Biochim. Biophys. Acta.* **1608**: 190-199.
- Hung, S.H., S.J. Chiu, L.Y. Lin, and R.L. Pan. 1995. Vacuolar H<sup>+</sup>-pyrophosphatase cDNA from etiolated mung bean seedlings. *Plant Physiol.* **109**: 1125-1127.
- Kane, P.M., C.T. Yamashiro, and T.H. Stevens. 1989. Biochemical characterization of the yeast vacuolar H<sup>+</sup>-ATPase. *J. Biol. Chem.* **264**: 19236-19244.
- Kim, E.J., R.G. Zhen, and P.A. Rea. 1995. Site-directed mutagenesis of vacuolar H<sup>+</sup>-pyrophosphatase. Necessity of Cys634 for inhibition by maleimides but not catalysis. *J. Biol. Chem.* **270**: 2630-2635.
- Laemmli, U.K. 1970. Cleavage of structural proteins during the assembly of the head of bacteriophage T4. *Nature* **227**: 680-685.
- Lanfermeijer, F.C., K. Venema, and M.G. Palmgren. 1998. Purification of a histidine-tagged plant plasma membrane H<sup>+</sup>-ATPase expressed in yeast. *Protein Expr. Purif.* **12**: 29-37.
- Larson, E., B. Howlett, and A.T. Jagendorf. 1986. Artificial reductant enhancement of the Lowry method for protein determination. *Anal. Biochem.* **155**: 243-248.
- Lin, H.H., Y.J. Pan, S.H. Hsu, R.C. Van, Y.Y. Hsiao, J.H. Chen, and R.L. Pan. 2005. Deletion mutation analysis on C-terminal domain of plant vacuolar H<sup>+</sup>-pyrophosphatase. *Arch. Biochem. Biophys.* **442**: 206-213.
- Liu, W., Y. Kamensky, R. Kakkar, E. Foley, R.J. Kulmacz, and G. Palmer. 2005. Purification and characterization of bovine adrenal cytochrome *b*<sub>561</sub> expressed in insect and yeast cell systems. *Protein Expr. Purif.* **40**: 429-439.
- López-Marqués, R.L., J.R. Pérez-Castiñeira, M.J. Buch-Pedersen, S. Marco, J.L. Rigaud, M.G. Palmgren, and A. Serrano. 2005. Large-scale purification of the proton pumping pyrophosphatase from *Thermotoga maritima*: a "Hot-Solve" method for isolation of recombinant thermophilic membrane proteins. *Biochim. Biophys. Acta.* **1716**: 69-76.
- Maeshima, M. 1991. H<sup>+</sup>-translocating inorganic pyrophosphatase of plant vacuoles. Inhibition by Ca<sup>2+</sup>, stabilization by Mg<sup>2+</sup> and immunological comparison with other inorganic pyrophosphatases. *Eur. J. Biochem.* **196**: 11-17.
- Maeshima, M. 2000. Vacuolar H<sup>+</sup>-pyrophosphatase. *Biochim. Biophys. Acta.* **1465**: 37-51.
- Maeshima, M. and S. Yoshida. 1989. Purification and properties of vacuolar membrane proton-translocating inorganic

- pyrophosphatase from mung bean. *J. Biol. Chem.* **264**: 20068-20073.
- McIntosh, M.T. and A.B. Vaidya. 2002. Vacuolar type H<sup>+</sup> pumping pyrophosphatases of parasitic protozoa. *Int. J. Parasitol.* **32**: 1-14.
- Mimura, H., Y. Nakanishi, M. Hirono, and M. Maeshima. 2004. Membrane topology of the H<sup>+</sup>-pyrophosphatase of *Streptomyces coelicolor* determined by cysteine-scanning mutagenesis. *J. Biol. Chem.* **279**: 35106-35112.
- Nakanishi, Y., T. Saijo, Y. Wada, and M. Maeshima. 2001. Mutagenic analysis of functional residues in putative substrate-binding site and acidic domains of vacuolar H<sup>+</sup>-pyrophosphatase. *J. Biol. Chem.* **276**: 7654-7660.
- Obermeyer, G., A. Sommer, and F.W. Bentrup. 1996. Potassium and voltage dependence of the inorganic pyrophosphatase of intact vacuoles from *Chenopodium rubrum*. *Biochim. Biophys. Acta.* **1284**: 203-212.
- Rea, P.A., Y. Kim, V. Sarafian, R.J. Poole, J.M. Davies, and D. Sanders. 1992. Vacuolar H<sup>+</sup>-translocating pyrophosphatases: a new category of ion translocase. *Trends Biochem. Sci.* **17**: 348-353.
- Rea, P.A. and R.J. Poole. 1993. Vacuolar H<sup>+</sup>-translocating pyrophosphatase. *Ann. Rev. Plant Physiol. Plant Mol. Biol.* **44**: 157-180.
- Takasu, A., Y. Nakanishi, T. Yamauchi, and M. Maeshima. 1997. Analysis of the substrate binding site and carboxyl terminal region of vacuolar H<sup>+</sup>-pyrophosphatase of mung bean with peptide antibodies. *J. Biochem. (Tokyo)* **122**: 883-889.
- Tzeng, C.M., C.Y. Yang, S.J. Yang, S.S. Jiang, S.Y. Kuo, S.H. Hung, J.T. Ma, and R.L. Pan. 1996. Subunit structure of vacuolar proton-pyrophosphatase as determined by radiation inactivation. *Biochem. J.* **316(Pt 1)**: 143-147.
- Walker, R.R. and R.A. Leigh. 1981. Mg<sup>2+</sup>-dependent, cation-stimulated inorganic pyrophosphatase associated with vacuoles isolated from storage roots of red beet (*Beta vulgaris* L.). *Planta* **153**: 150-155.
- Wu, J.J., J.T. Ma, and R.L. Pan. 1991. Functional size analysis of pyrophosphatase from *Rhodospirillum rubrum* determined by radiation inactivation. *FEBS Lett.* **283**: 57-60.
- Yang, S.J., S.S. Jiang, Y.Y. Hsiao, R.C. Van, Y.J. Pan, and R.L. Pan. 2004. Thermoinactivation analysis of vacuolar H<sup>+</sup>-pyrophosphatase. *Biochim. Biophys. Acta.* **1656**: 88-95.
- Yang, S.J., S.S. Jiang, S.Y. Kuo, S.H. Hung, M.F. Tam, and R.L. Pan. 1999. Localization of a carboxylic residue possibly involved in the inhibition of vacuolar H<sup>+</sup>-pyrophosphatase by *N, N'*-dicyclohexylcarbodiimide. *Biochem. J.* **342(Pt 3)**: 641-646.
- Yang, S.J., S.S. Jiang, C.M. Tzeng, S.Y. Kuo, S.H. Hung, and R.L. Pan. 1996. Involvement of tyrosine residue in the inhibition of plant vacuolar H<sup>+</sup>-pyrophosphatase by tetranitromethane. *Biochim. Biophys. Acta.* **1294**: 89-97.
- Yang, S.J., S.S. Jiang, R.C. Van, Y.Y. Hsiao, and R.L. Pan. 2000. A lysine residue involved in the inhibition of vacuolar H<sup>+</sup>-pyrophosphatase by fluorescein 5'-isothiocyanate. *Biochim. Biophys. Acta.* **1460**: 375-383.
- Zhen, R.G., E.J. Kim, and P.A. Rea. 1994. Localization of cytosolically oriented maleimide-reactive domain of vacuolar H<sup>+</sup>-pyrophosphatase. *J. Biol. Chem.* **269**: 23342-23350.
- Zhen, R.G., E.J. Kim, and P.A. Rea. 1997. Acidic residues necessary for pyrophosphate-energized pumping and inhibition of the vacuolar H<sup>+</sup>-pyrophosphatase by *N, N'*-dicyclo-hexylcarbodiimide. *J. Biol. Chem.* **272**: 22340-22348.

# 酵母菌表現組胺酸尾飾液泡焦磷酸水解酶之純化、定性、以及光譜分析

徐慎行<sup>1</sup> 蕭義勇<sup>2,3</sup> 劉佩芬<sup>1</sup> 林士鳴<sup>1</sup> 羅悅瑜<sup>1</sup> 潘榮隆<sup>1</sup>

<sup>1</sup> 國立清華大學 生物資訊與結構生物研究所

<sup>2</sup> 國立東華大學 海洋生物科技研究所

<sup>3</sup> 國立海洋生物博物館

液泡無機焦磷酸水解酶 (V-PPase) 利用水解焦磷酸產生能量來驅動質子傳遞造成細胞膜內外的質子梯度，而 V-PPase 水解及質子傳遞的活性可被許多的離子所調控，相對高濃度的 K<sup>+</sup> 可以促進 V-PPase 的活性而 F<sup>-</sup>、Na<sup>+</sup>、Ca<sup>2+</sup> 以及過多的 PP<sub>i</sub> 則會抑制它的活性，在本研究中我們利用酵母菌表達系統表達帶有六個組胺酸尾飾的 V-PPase 接著利用 n-dodecyl β-D-maltoside (DDM) 當作介面活性劑來將 V-PPase 由細胞膜中溶解出來，再利用 Ni<sup>2+</sup>-NTA 親合性層析管注將 V-PPase 純化出來得到一個分子量大約是 73 kDa 的純化蛋白質，組胺酸尾飾 V-PPase 的水解活性大約是 86.4 ± 7.4 μmol PP<sub>i</sub>/mg.h 比在細胞膜上的還要高約 6.5 倍；比較酵母菌表達的組胺酸尾飾 V-PPase 的活性只有直接由綠豆中純化出來的 59%。進一步的分析組胺酸尾飾 V-PPase 的特性，發現純化的 V-PPase 和位在細胞膜上的有相似的特性。再則，利用光譜分析純化的組胺酸尾飾 V-PPase，發現影響 V-PPase 活性的這些離子多會造成 V-PPase 結構上的改變 (特別是二級結構的改變)；這個結果證實影響 V-PPase 的離子是經由改變其構型 (二級結構) 來影響其活性。

**關鍵詞：** 圓二色譜學；金屬親合性層析；液泡焦磷酸水解酶；液泡。

